Available online www.jocpr.com

Journal of Chemical and Pharmaceutical Research, 2015, 7(9):133-143

Research Article

ISSN : 0975-7384
CODEN(USA) : JCPRC5

Growth and characterization of L-proline potassium bromide: A semiorganic NLO crystal

V. Vasantha Kumari[1], P. Selvarajan[2] and R. Thilagavathi[1]

[1]Department of Physics, Govindammal Aditanar College for Women, Tiruchendur, Tamil Nadu, India
[2]Department of Physics, Aditanar College of Arts & Science, Tiruchendur, Tamil Nadu, India

---

ABSTRACT

Single nonlinear optical crystals of L-Proline Potassium Bromide (LPPB) were synthesized and grown by dissolving L - proline and potassium bromide in 1:1 molar ratio using deionized water as the solvent. The crystal parameters of the grown crystals have been evaluated by single crystal and powder XRD methods. Optical spectral studies have been carried out to find the band gap and optical constants of the material. Second Harmonic Generation (SHG) study reveals the nonlinear optical (NLO) property of sample. Mechanical strength of the grown samples is tested by hardness studies. TG/DTA studies were carried out to confirm the thermal stability to the grown crystals. EDAX test was also carried out to test the presence of elements in the sample. The details of the method adopted for crystal growth and the results obtained through various characterizations are analyzed and interpreted in detail.

Keywords: Crystal Growth; Solution method; Characterization; FTIR; TG/DTA; microhardness; SHG

INTRODUCTION

Nonlinear optical materials have attracted much attention because of their potential applications in the field of optical communications, high-speed information processing, optical data storage and in emerging optoelectronics technology [1, 2]. In earlier years, investigations were initially focused on purely inorganic materials, which were the first to demonstrate second-order nonlinear optical properties [3]. In recent years, much attention has been paid to the research of novel nonlinear optical NLO) materials, especially semiorganic crystals. Semiorganic compounds illustrate the following features:(i) dipolar structure composed of an electron donating and electron accepting group (ii) the contribution from the delocalized π electrons belonging to organic ligand results in high nonlinear optic and electro-optic coefficients in the semiorganic crystals also; (iii) the organic ligand is ionically bonded to metal ion to impart improved mechanical and thermal properties; (4) exhibit wider transparency range, chemical stabilities and bulk crystal morphologies. Optical nonlinearity of the crystals with O−H bond has been extensively studied [4–8]. Proline is an abundant amino acid in collagen and is exceptional among the amino acids because it is the only one in which the amino group is a part of a pyrrolidine ring, making it rigid and directional in biological systems [9]. Single crystals of L-proline shows no centre of symmetry and its NLO coefficient have been examined by Boomadevi and Dhanasekaran [10]. Also Kandasamy et al. [11], have grown L-Proline cadmium chloride monohydrate (LPCCM) and reported that the second harmonic generation efficiency of their crystal was twice that of KDP. And also some L-proline-based materials have been reported [12, 13]. In the present investigation we report on the synthesis and growth of LPPB from using deionized water as the solvent and its characterization. Presently, crystals of L-proline potassium bromide (LPPB) have been studied.

EXPERIMENTAL SECTION

The grown crystals were subjected to Single Crystal X-ray diffraction studies using ENRAF NONIUS X-ray diffractometer with MoK_α (λ=0.71069Å) radiation to evaluate the lattice parameter values. The grown LPPB crystal

was crushed to a uniform fine powder and subjected to powder X-ray diffraction using a powder X -ray diffractometer (PANalatyical Model, Nickel filtered Cu Kα radiations with λ=1.54056 Å at 35 kV,10 mA) to identify the reflection planes and hence the crystal parameters. The Fourier transform infrared spectrum of LPPB was recorded in the region 400-4000 cm^{-1} with SHIMADZU spectrometer using KBr pellet containing LPPB powder obtained from the grown crystal. The transmission properties of the crystals were examined using VARIAN CARY 5E UV - Vis - NIR spectrometer in the range 190 nm to 1100 nm. The EDAX analysis of the grown LPPB crystals was carried out using Jeol 6390LV model scanning electron microscope. The Thermo Gravimetric (TG) analysis of the sample is tested using TGA Q500 V20.10 Build 36 thermal analyser by heating the sample at a rate of 10 K min^{-1} in inert nitrogen atmosphere. To confirm the nonlinear optical property Kurtz and Perry powder SHG test was carried out using Nd: YAG Q-switched laser which emits the first harmonic output of 1064 nm. Microhardness analysis was carried out using Vickers microhardness tester fitted with a diamond indenter.

RESULTS AND DISCUSSION

3.1 Synthesis and solubility

The commercially available 99% pure L-proline and potassium bromide were used in this work to grow single crystals of L-proline potassium bromide (LPPB). The salt of LPPB was synthesized by taking L-proline and potassium bromide in the molar ratio 1:1. Since the mixture is readily soluble in water, deionised water is used as the solvent. Calculated amounts of the chemicals were dissolved in deionized water and stirred well using a magnetic stirrer for about 2 hours. The solution was heated until the synthesized salt of LPPB was obtained. During synthesis, temperature of the solution was maintained at 50^{o}C in order to avoid oxidation of the sample. The purity of the synthesized salt was improved by repeated re-crystallization. The L- proline potassium bromide compound was formed as per the following equation.

$$C_5H_9NO_2 + KBr \rightarrow C_5H_9NO_2\ KBr \qquad (1.1)$$

The solubility of the solute can be determined by dissolving the solute in the solvent maintained at a constant temperature with continuous stirring. On reaching saturation, equilibrium concentration of the solute can be determined gravimetrically [14] and the solubility is calculated at different temperatures. The solubility curve of LPPB is plotted in figure 1. It is observed that solubility increases with temperature which shows that the temperature coefficient of solubility is positive.

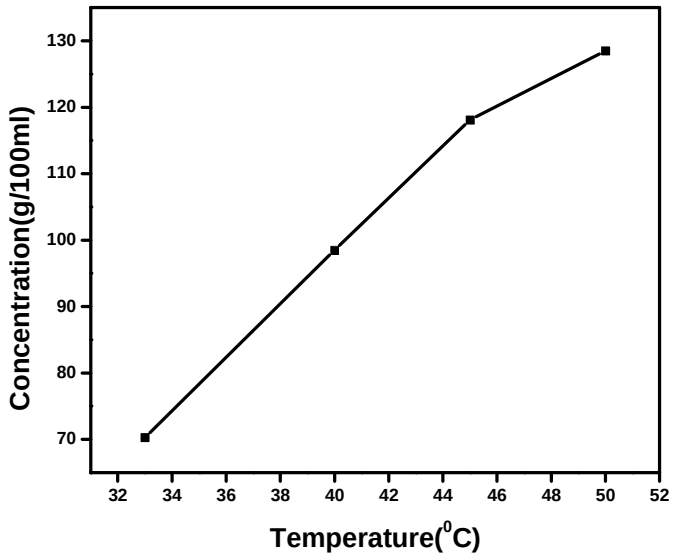

Fig. 1 Solubility curve of LPPB sample

3.2. Crystal growth

As per the solubility data, the saturated solution of LPPB was prepared using deionised water as solvent and the contents were stirred well using a temperature – controlled magnetic stirrer to yield a homogeneous solution. The solution was filtered using Whatman filter paper. The filtered solution was then kept in a crystal growth vessel closed with a perforated sheet for slow evaporation at room temperature. Transparent, colourless crystal of size (7 × 6 ×4) mm^3 was obtained within a period of 15 days. The photograph of the grown crystal is shown in figure 2.

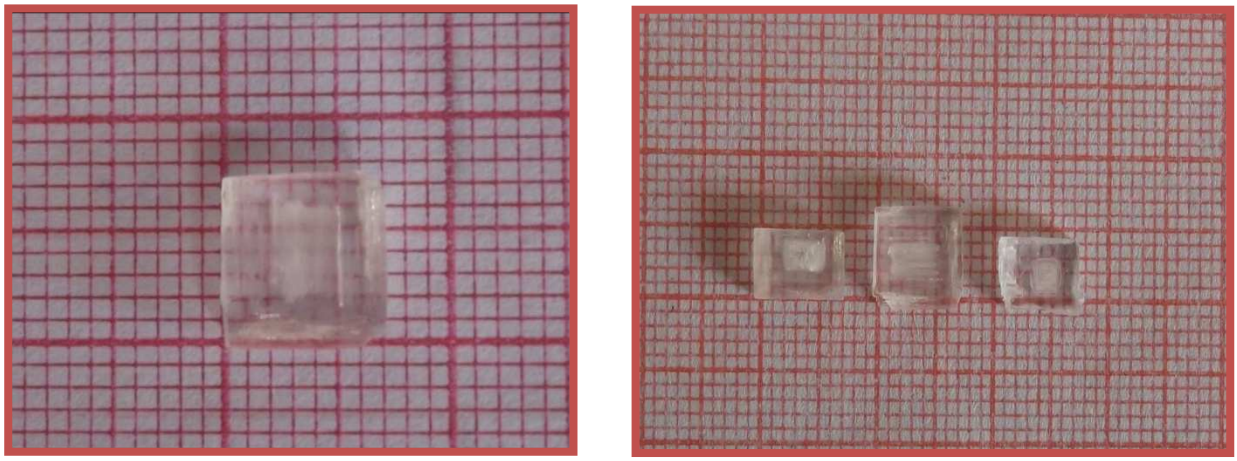

Fig. 2 Photograph of LPPB crystal

3.3 Single crystal XRD studies

Single crystal X- ray diffraction analysis for the grown crystal has been carried out to identify the cell parameters using ENRAF NONIUS CAD-4 automatic X-ray diffractometer. The single crystal XRD data of the grown crystal is presented in Table 1.

Table 1: Crystallographic data of LPPB crystal

Molecular formula for LPPB	$C_5H_9NO_2KBr$
Molecular weight	234.14 g/ml
Symmetry	Hexagonal
Space group	P6
Cell parameters	a = 4.662 Å b = 4.662 Å c = 22.90 Å $\alpha = \beta = 90^o$, $\gamma = 120^o$
Volume	431 $Å^3$
Crystal Color	Colourless , transparent

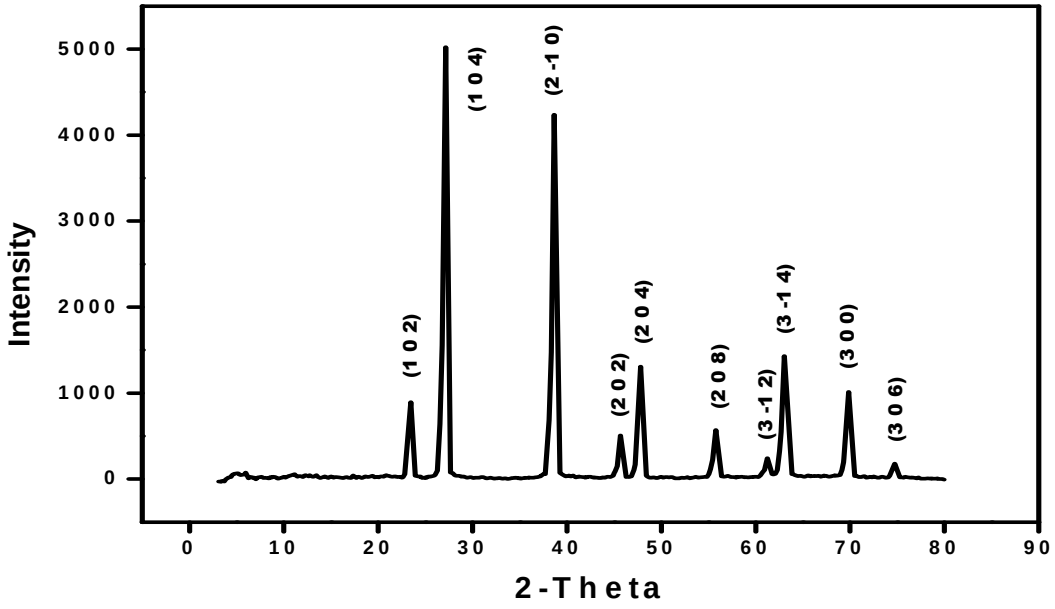

Fig. 3 Powder XRD Pattern of LPPB

Table 2: d, 2θ, h k l values and relative intensity of LPPB

Peak. No.	2θ(degree)	d-spacing (Å)	h k l	Relative Intensity
1	23.443	3.79167	1 0 2	17.8
2	27.122	3.28517	1 0 4	100
3	38.641	2.32825	2 -1 0	84.4
4	45.667	1.98544	2 0 2	10.1
5	47.779	1.90210	2 0 4	26
6	55.759	1.64730	2 0 8	11.4
7	61.245	1.51223	3 -1 2	4.9
8	63.010	1.47406	3 -1 4	28.5
9	69.841	1.34564	3 0 0	20.2
10	74.730	1.26926	3 0 6	3.6

3.4 Powder XRD studies

The grown LPPB crystal has been crushed to a uniform fine powder and subjected to powder X-ray diffraction to identify the reflection planes and hence the crystal parameters. The powder X-ray diffraction pattern of LPPB crystal is shown in figure 3. All the reflections of powder XRD pattern were indexed using the INDEXING SOFTWARE package. The obtained h k l values, 2θ and d-spacing are presented in Table 2. The lattice parameters from powder XRD data were found using UNITCELL software package and the obtained values are found to be a = 4.662 Å, b = 4.662 Å, c = 22.90 Å, and volume = 431 $Å^3$. The obtained values are found to be in agreement with the experimental values.

3.5 FTIR Spectral analysis

The FTIR spectrum was recorded to understand the chemical bonding, and it provides useful information regarding the molecular structure of the compound [15]. FTIR spectrum was taken for the powdered sample in the wavelength range 4000–400 cm^{-1} as shown in Figure 4. The strong band at 3427.62 cm^{-1} corresponds to O-H stretching. The peak observed at 2364.81 cm^{-1} is due to the combination overtone bands. The sharp peak observed at 1627.97 cm^{-1} is due to the NH_2^+ in-plane deformation. The COO^- symmetric stretching is observed at 1406.15 cm^{-1} and the C-H deformation occurs at 1386.88 cm^{-1}. The rocking of CH_2 group is assigned at 1024.24 cm^{-1} and the peak observed at 673.18 cm^{-1} is due to the C-Br stretching. The rocking vibration of COO^- occur at 617.24 cm^{-1}. The peak at 466.79 cm^{-1} is due to the NH_3^+ torsion. The functional group assignments are made from the standard references [16-18]. The spectral assignments are provided in table 3.

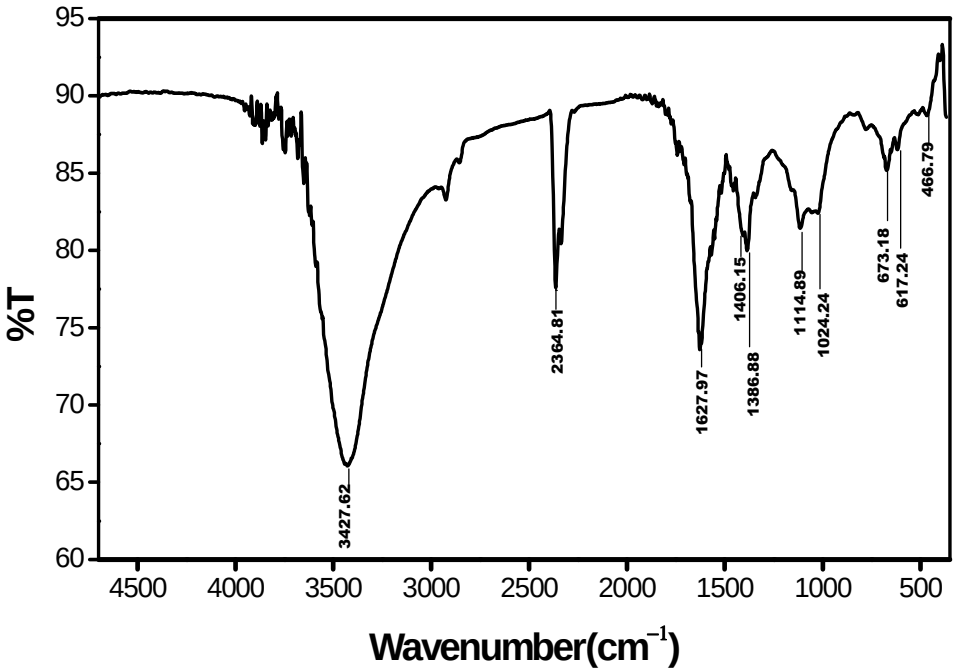

Fig. 4 FTIR spectrum of LPPB

Table 3: FTIR Spectral assignments of LPPB

Wave number (cm^{-1})	Assignments
3427.63	O-H Stretching and NH_3^+ stretching
2364.81	Combination overtone bonds
1627.97	NH_2 in-plane deformation
1406.15	COO^- stretching
1386.88	C-C stretching
1024.24	CH_2 rocking
673.18	C-Br stretching
617.24	COO^- rocking vibration
466.79	NH_3^+ torsion

3.6 EDAX Studies

Energy Dispersive X- ray spectroscopy (EDAX) is an analytical technique used for the elemental analysis of the sample. The EDAX spectrum of the LPPB sample taken using a computer controlled scanning electron microscope is displayed in figure 5.

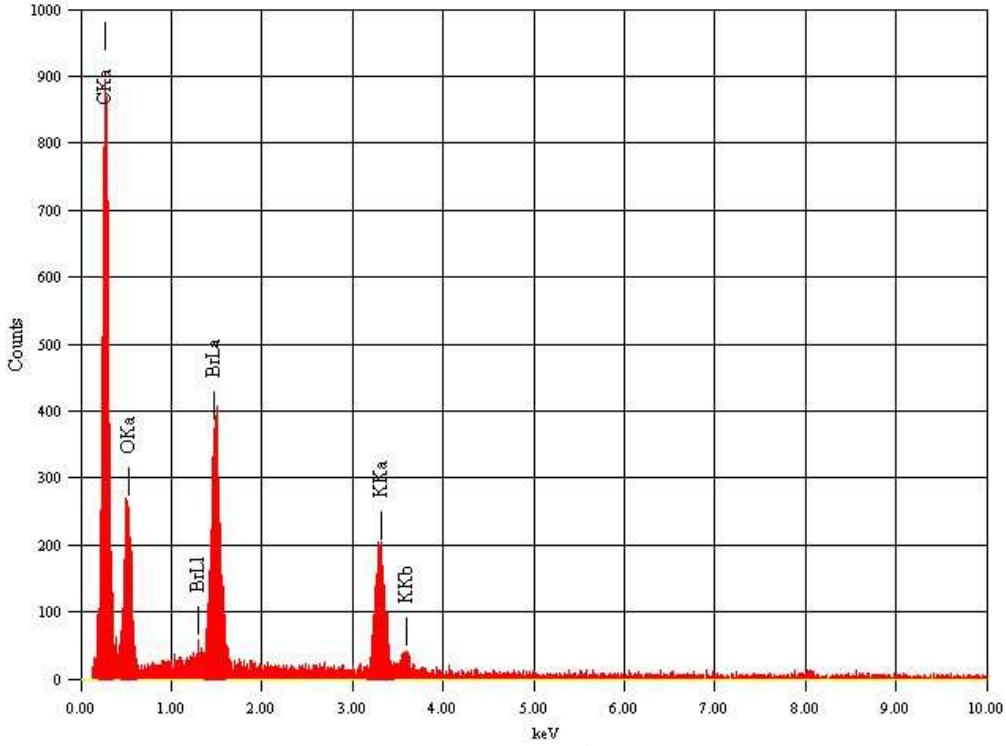

Fig. 5 EDAX Spectrum of LPPB

From the spectrum it is confirmed that the elements such as C, O, K and Br were present in the sample. The element hydrogen cannot be identified using the EDAX technique (table 4).

Table 4 EDAX data of LPPB

Element	(k eV)	Mass %	Atom %
C K	0.277	60.6	84.61
O K	0.525	6.66	6.98
K K	3.312	7.05	3.02
Br L	1.48	25.7	5.39

3.7 Thermo gravimetric analysis

The thermal stability of LPPB was studied by thermogravimetric analysis (TGA) and differential thermal analysis (DTA) at a heating rate of 10 $^{\circ}C\ min^{-1}$ in inert nitrogen atmosphere. The resulting TGA/DTA trace is shown in figure 6. In practice, a small sample weight is desirable for thermo gravimetric results [19] and hence the weight of the sample taken for investigation is 7.937 mg. The initial mass of the sample is 7.937 mg. There is slight change in mass upto a temperature of 310^{o}C. At 310^{o} C there is a single stage weight loss. This may be due to the thermal decomposition of the sample. After 310^{o} C there is a gradual and marginal weight loss of 3 % upto 700^{o}C.

Moreover even at 700° C, 95 % of the sample is retained. This shows high thermal stability of the grown LPPB crystal which is a prerequisite quality for device fabrication.

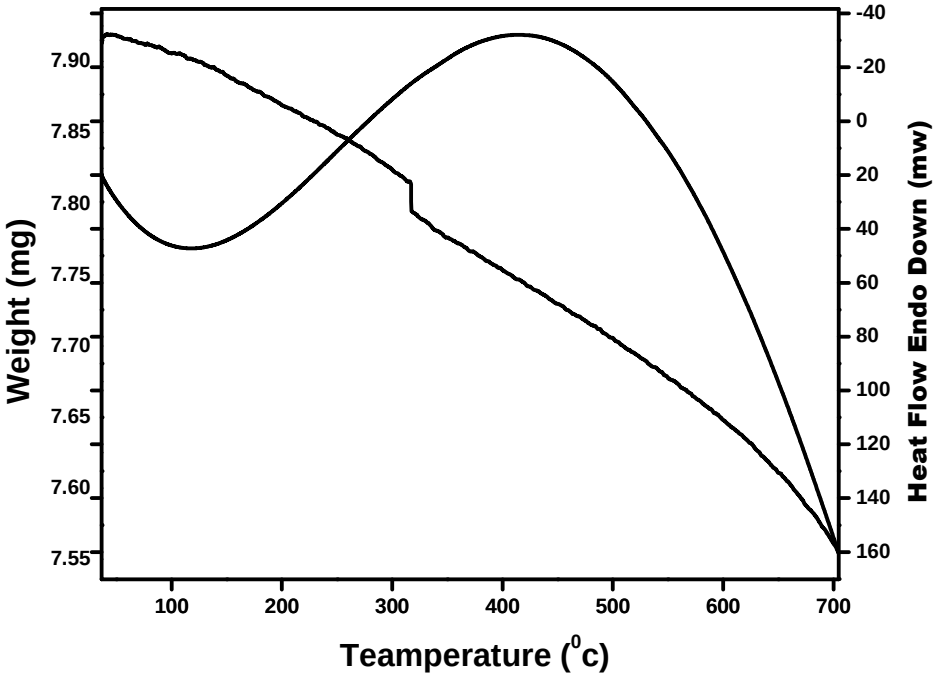

Fig. 6 TGA/DTA curves of LPPB

3.8 Optical Transmission analysis

UV-Visible spectral analysis gives useful information about electronic transitions in the compound [20]. The UV-Vis-NIR transmission spectrum plays a vital role in identifying the potential of a NLO material because a given NLO material can be of utility only if it has a wide transparency window without any absorption at the fundamental and second harmonic wavelengths. It is also useful for obtaining information about the structure of the molecule because, the absorption of UV and visible light involves promotion of the electron in the σ and π orbital from the ground state to higher states [21, 22]. The optical behavior of LPPB crystal was analyzed using a VARIAN CARY 5E UV-Vis spectrophotometer in the wavelength range of 190–2200 nm. For this study, an optically polished single crystal of thickness 1.5 mm was used and the recorded transmittance spectrum is shown in figure 7. The cut-off wavelength of the crystal is observed at 234 nm, and the crystals show good transmittance percentage of 76.9 % in the range of 234–1400 nm. For optical fabrications, the crystal should be highly transparent in the considered region of wavelength [23, 24]. It is also an important requirement for NLO materials having nonlinear optical applications [25]. There is no absorption in the entire visible region of the electromagnetic spectrum. Favourable transmittance of the crystal in the entire visible region suggests its suitability for second harmonic generation [26].

The band gap E_g is evaluated using extrapolation of the linear part [27], in the high energy region. The energy dependence of absorption coefficient suggests the occurrence of direct band gap of the crystal obeying the following equation for high photon energies (hν)

$$(\alpha h \nu)^2 = A (E_g - h\nu) \qquad (1.2)$$

where E_g is the optical band gap of the crystal and A is a constant. The variation of $(\alpha h \nu)^2$ with hν in the fundamental absorption region are plotted in figure 8. The band gap of the crystal can be evaluated by extrapolation of the linear part to zero absorption which is found to be 5.39 eV. As a consequence of a wide band gap, the grown crystal has a large transmittance in the visible and near infrared region [28] and the crystal can be a suitable material for the optoelectronic devices like LED and laser diodes [29].

Hence by tailoring the absorption coefficient and tuning the band gap of the material, we can achieve the desired material suitable for fabricating various layers of optoelectronic devices.

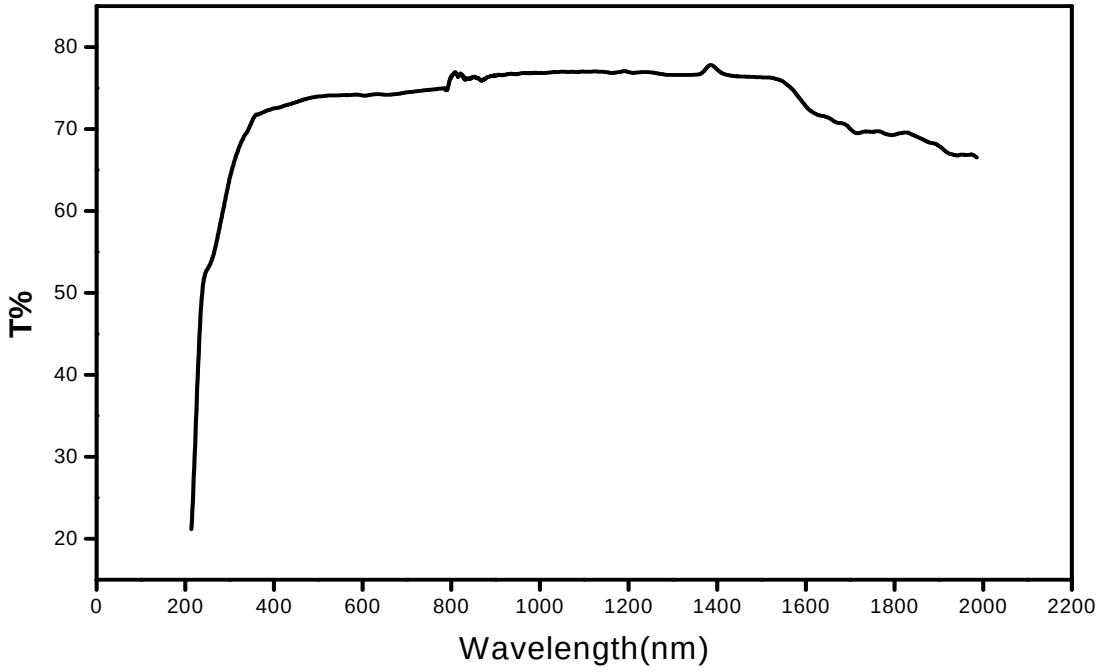

Fig. 7 Transmittance Spectrum of LPPB Crystal

3.9 Determination of optical constants

The optical behavior of materials is important to determine their usage in a material such as refractive index and extinction coefficient is quite essential to examine the material's potential optoelectronic applications [30]. Further, the optical properties may also be closely related to the material's atomic structure, electronic band structure and electrical properties. The optical constants (K, n) were determined from the transmission (T) and reflection (R) spectrum based on the following relations.

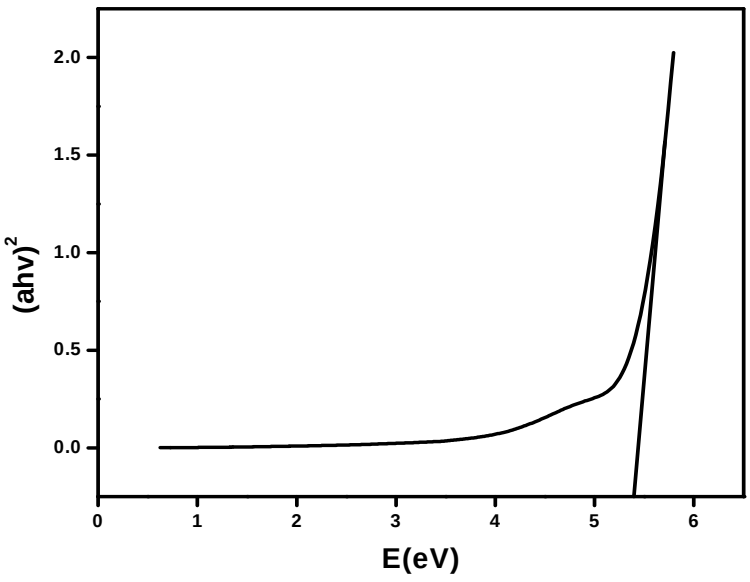

Fig.8 Plot of $(\alpha hv)^2$ versus E (eV)

The extinction coefficient K is expressed as [31]

$$K = \frac{\lambda \alpha}{4\pi} \quad (1.3)$$

The reflectance gives the ratio of the energy of reflected to incident light from a crystal. The reflectance in terms of the absorption coefficient can be calculated using [32]

$$R = 1 \pm \frac{(1-exp(-\alpha t)+exp(\alpha t))^{\frac{1}{2}}}{1+exp(-\alpha t)} \quad (1.4)$$

The refractive index (n) can be determined from the reflectance using

$$n = \frac{\sqrt{R}-1}{\sqrt{R}+1} \quad (1.5)$$

From the graph (Fig.9) it is clear that the extinction coefficient (K), reflectance (R) and refractive index (n) vary with wavelength and hence depend on the photon energy. The internal efficiency also depends on the photon energy. Hence by tailoring the photon energy, one can achieve the desired material for the device fabrication.

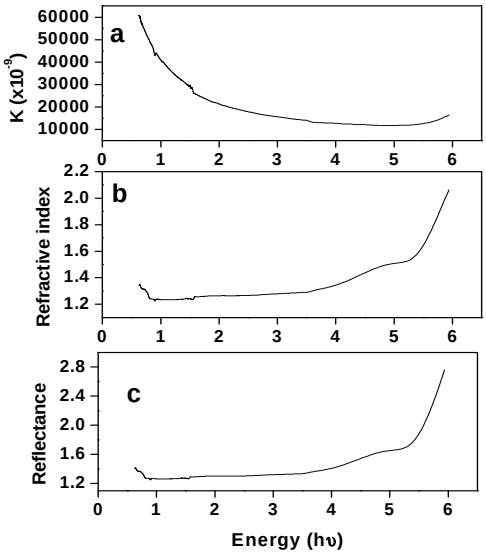

Fig .9 Optical Transmittance of LPPB

3.10 Vickers microhardness test

Hardness is measure of resistance of the material to plastic deformation. The hardness of the material plays a significant role in device fabrication. The hardness of the crystal carries information about the mechanical strength and molecular binding of the material. Recently, there is an increasing demand for exploring new electro-optic materials having simple structure. The measurement of hardness is very important as far as the fabrication of devices is concerned. Measurement of hardness is a useful non-destructive testing method to determine the bond strength [33].

Microhardness analysis was carried out for the grown crystal using Vickers microhardness tester fitted with a diamond indenter. A well polished LPPB crystal of 2 mm thick was placed on the platform on the Vickers microhardness tester and the loads of different magnitude were applied over a fixed interval of time and the hardness was calculated using the relation

$$H_v = 1.8544\ P/\ d^2\ (kg/mm^2) \quad (1.6)$$

Where P is the applied load (kg) and d is the diagonal length of the indentation impression (mm). The variation of H_v with the applied load P is shown in figure 10. The microhardness correlates with other mechanical properties such as elastic constant and yield strength [34] during an indentation process, the external work applied by the indenter is converted into a strain energy component proportional to the volume of the resultant impression and a surface energy component proportional to the area of the resultant impression. Microhardness is a general microprobe for assessing the bond strength, apart being a measure of bulk strength.

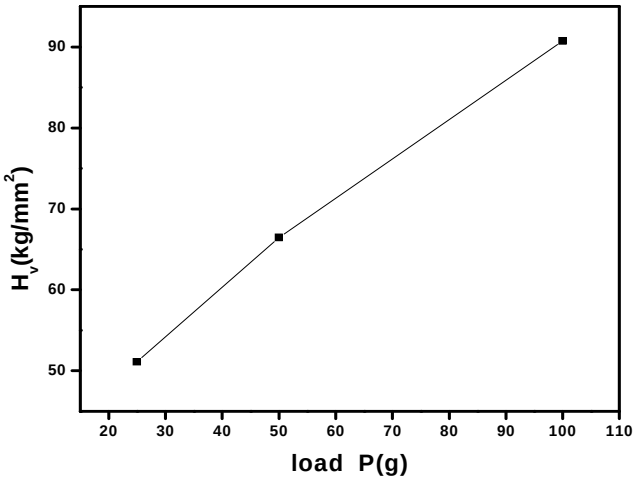

Fig. 10 H_v versus Load P

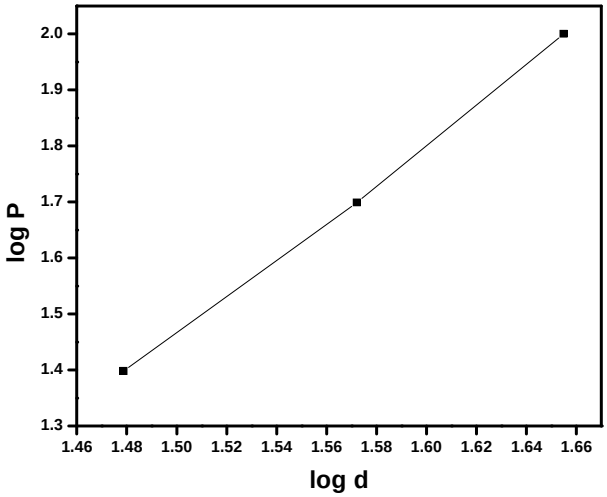

Fig. 11 log P versus log d

H_v increases with increasing load which shows that LPPB crystal exhibits Reverse Indentation Size Effect (RISE). A plot of log P versus log d for the grown crystal is shown in figure 11. The plot yields a straight line graph, and its slope gives the work hardening coefficient n. According to Onitsch [35] n lies between 1 and 1.6 for hard materials and is greater than 1.6 for soft materials [36]. The 'n' value observed in the present studies is around 3.413 suggesting that the grown LPPB crystal is a relatively softer material.

According to Meyer's relation

$$P = k_1 d^n \quad (1.7)$$

Where k_1 is the standard hardness value which can be obtained from the plot of P versus d^n which is found to be 4.087 is shown in figure 12.

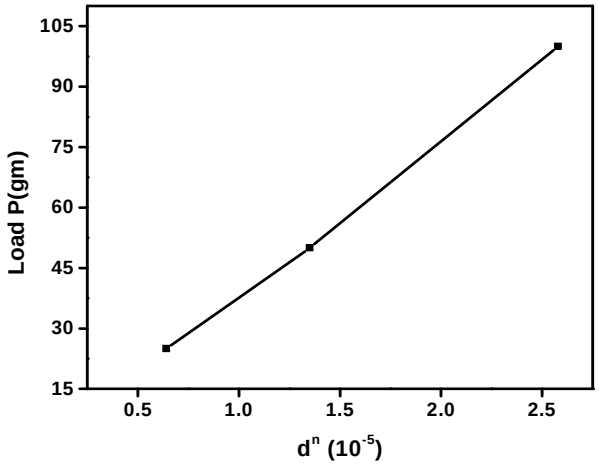

Fig. 12 load P vs. d^n

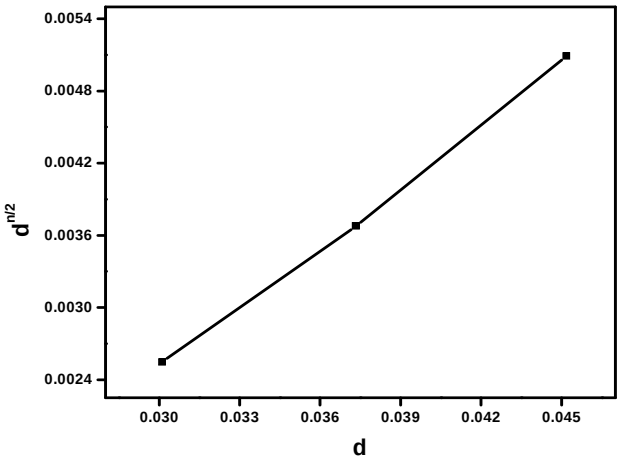

Fig. 13 Fig. $d^{n/2}$ vs. d

Since the material takes some time to revert to be elastic mode after deformation, correction x is applied to the d value and kick's law is related as.

$$P = k_2(d + x)^2 \quad (1.8)$$

From eqn (1.7) and eqn (1.8)

$$d^{n/2} = \left(\frac{k_2}{k_1}\right)^{1/2} d + \left(\frac{k_2}{k_1}\right)^{1/2} x \quad (1.9)$$

The slope of $d^{n/2}$ versus d yields $\frac{k_2}{k_1}^{1/2}$ and x is measured from the intercept as shown in figure 13.

The yield strength of the material can be found using the formula

$\sigma_v = H_v /3$ (1.10)

The load dependent hardness parameter n, k_1 and k_2 yield strength are calculated for minimum load for the grown LPPB crystal and the values are shown in Table 5.

Table 5 Hardness parameter of the LPPB Crystal

n	k_1 (kg/mm^2)	k_2 (kg/mm^2)	x	σ_v (MPa)
3.4130	11+.8	11.6	0.015	166.92

The elastic stiffness constant is a measure of the resistance of the material to deformation. The elastic stiffness constant (C_{11}) for different loads are calculated using Wooster's empirical formula $C_{11}=H_v^{7/4}$ and is shown in table 6. The stiffness constant gives an idea about the tightness of bonding with the neighbouring atoms. In the case of LPPB crystal, the stiffness constant is found to increase with the applied load.

Table 6 Elastic stiffness constant for different loads

Load (g)	C_{11} (10^{14}MPa)
25	1.01
50	1.57
100	2.63

3.11 SHG measurement

The microscopic origin of non-linearity in the NLO materials is due to the presence of delocalized π-electron systems, connecting donor and accepter groups, which enhance their asymmetric polarizability. Each type of constituent chemical bond is regarded as one part of the whole crystal that has contributions to the total nonlinearity. The distribution of valence electrons of the metallic elements is an important factor that strongly affects the linear and nonlinear properties of each type of constituent chemical bond [37]. Second harmonic generation (SHG) test is important to check whether a sample is NLO active or not and it was carried out by powder Kurtz and Perry technique [38]. The crystal was ground into a homogenous powder and densely packed between two transparent glass slides. A Q- Switched Nd: YAG laser beam of wavelength 1064 nm (pulse width 6 ns) was allowed to strike the sample cell normally. With this source radiation, the generation of second harmonics was confirmed by the emission of green light from the sample. Second harmonic output of 4.2 mJ was obtained for an input energy of 0.68 J. A sample of powdered Potassium dihydrogen phosphate (KDP) was used as the reference material in the SHG measurement and the output was found to be 8.8 mJ. The relative SHG efficiency for LPPB Crystal is found to be 0.47 times that of KDP sample.

CONCLUSION

Single crystals of L- Proline Potassium Bromide (LPPB) were successfully grown by slow evaporation solution grown technique. L-proline crystallizes in Hexagonal structure. Powder XRD studies shows crystalline nature of LPPB crystal. The presence of functional groups in the crystal is confirmed from the FTIR studies. EDAX spectrum confirmed the elements present in the sample. The band gap is determined from UV-Vis-NIR studies as E_g=5.39 eV. Thermo Gravimetric analysis shows that LPPB crystals are thermally stable. Microhardness analysis reveals that LPPB belongs to soft material category. The second harmonic efficiency (SHG) of LPPB was tested using powder Kurtz- Perry method and the SHG efficiency of LPPB is found to be 0.47 times that of the standard KDP.

Acknowledgments

The authors would like to thank the staff members of RRL (Trivandrum), CECRI (Karaikkudi), Crescent Engineering College (Chennai), St. Joseph's College (Trichy), STIC, Cochin and M.K. University (Madurai) for having helped us to carry out the research work. Also we thank authorities of Management of Aditanar College of Arts and Science, Tiruchendur, Govindammal College for Women, Tiruchendur and S.T. Hindu College, Nagercoil for the encouragement given to us to carry out the research work.

REFERENCES

[1] Eaton; F David, *Nonlinear Optical Materials*, **1991**, 253, 281-287.
[2] VG Dmitriev, GG Gurzadyan, DN Nikgosyan. Hand Book of Nonlinear Optical Crystals, 2nd Edition, Springer, New York, **1997**.
[3] PA Franken; AE Hill; CW Peters; G Weinreich, *Phys. Rev. Lett.*, **1961**, 7, 118-119.
[4] D Xu; D Xue, *J, Cryst. Growth*, **200**8,310, 1385-1390.
[5] X Ren; D Xu; D Xue, *J. Cryst. Growth*, **2008,** 310, 2005–2009.
[6] D Yu; D Xue; H Ratajczak, *J. Mol. Struct.*, **2006**, 280, 792–793.
[7] D Yu; D Xue; H Ratajczak, *Phys. B: Condens. Mater***. 2006,** 371 (1), 170-176.
[8] D Xu; D Xue, *J. Cryst. Growth*, **2006,** 286, 108-113.
[9] S Myung; M Pink; M H Baik; David E Clemmer, *Acta Crystallogr.*, **2005**, C 61, 506-508.
[10] S Boomadevi; R Dhanasekaran, *J. Crystal Growth*, **2004**, 261, 70-76.
[11] A Kandasamy; R Siddeswaran; P Murugakoothan; P. Suresh Kumar; R Mohan, *Cryst. Growth Des.* **2007**, 7, 183-186.
[12] T Uma Devi; N Lawrence; R Ramesh Babu; K Ramamurthi, *J. Crystal Growth*, **2008**, 310, 116-123.
[13] SA Martin Britto Das; S Natarajan, *Cryst. Res. Technol*., **2007**, 42, 471-476.
[14] P Selvarajan; J Glorium Arul Raj; SPerumal, *J.Crystal Growth*, **2009**, 311, 3835-3840.
[15] S Sudhahar; M Krishna Kumar; A Silambarasan; R Muralidharan; R Mohan Kumar, *Journal of Materials*, **2013**, 539312.
[16] J Thomas Joseph Prakash; S kumararaman, *Materials letters*, 2008, 62, 4097-4099.
[17] S Boomadevi; R Dhanasekaran, *J. Cryst. Growth*, **2004**, 261, 70-76.
[18] P Paramasivam; C Ramachandra Raja, *J. of Crystallization process and Technolog.*, **2012,** 2 21-24.
[19] G H Jeffery,J Bassett,J Mendham, RC Denney. Vogul's Text Book of Quantitative Chemical Analysis, ELIBS, Addison Wesley Longman Limited, UK, 1989.
[20] CNR Rao, Ultraviolet and Visible Spectroscopy, Butterworths, 3rd Edition, London, 1975.
[21] V Subhashini; S Ponnusamy; CM Chelvan, *Journal of Crystal Growth*, **2010**, 312(7), 1040-1045.
[22] T Baraniraj; P Philominathan, *Journal of Crystal Growth*, **2009,** 311, 3849-3854.
[23] VKrishnakumar; R Nagalakshmi, *Spectrochimica Acta Part A*., **2005,** 61, 499-507.
[24] V Krishnakumar; R John Xavier, *Spectrochimica Acta Part A*., **2004**, 60, 709-714.
[25] N Vijayan; RR Babu; M Gunasekaran; R Gopalakrishnan; P Ramasamy; R Kumaresan; CW Lan, *Journal of Crystal Growth*, **2003**, 249, 309-315.
[26] SA Roshan; J Cyriac; MA Ittyachen, *Mater. Lett.*, **2001**,49, 299-302.
[27] CA Kumar; D Kaur; R Chandra, *Opt. Mater*., **2007**, 29, 995-998.
[28] DDO Eya; AJ Ekpunobi; CE Okeke, *Acad. Open Internet J*., **2006**, **17,** 1-10.
[29] K Kumar; K Ramamoorthy; PM Koinkar; R Chandramohan; K. Sankaranarayanan, *J. Cryst. Growth*, **2006**, 289, 405-407.
[30] M Dongol, *Egyptian Journal of Solids*, **2002**, 25(1), 33-47.
[31]BK Periyasamy; RS Jebas; N Gopalakrishnan; T Balasubramanian, *Mater. Lett*., **2007**, 61(21), 4246-4249.
[32] Jain John; P Christuraj; K Anitha; T Balasubramanian, *Materials Chemistry and Physics*, **2009**, 118, 284-287.
[33] R Rani Christu Dhas; J Benet Charles; FD Gnanam, *J.Cryst. Growth*, **1994**, 137, 295-298.
[34] Yu Ya Kharitonov; RL Davidovich; VI Kostin; LA Zemnukhova; VI Sengienko, *Russian J. Inorgan. Chem.*, **1972**, 17, 682-683.
[34] J Benet Charles; FD Gnanam, *Cryst. Res. Tech*., **1994**, 29, 707-712.
[35] EM Onitsch. Mikroscopia, 1947, 2, 131-134.
[36] S Karan; SPS Gupta, *Mater. Sci. Eng. A*, **2005**, 398, 198-203.
[37] DF Xue; SY zhang, *Physica B: Condensed Matter*., **1999**, 262, 78-83.
[38] SK Kurtz; TT Perry, *Journal of Applied Physics*, **1968**, 39(8), 3798-3813.